Liu et al. PhotoniX (2025) 6:7
https://doi.org/10.1186/s43074-025-00167-6

PhotoniX

RESEARCH Open Access

Suppression of local decay rate through energy quantum confinement effect in non-Markovian waveguide QED

Yuan Liu[1], Hong-Bo Sun[1,2*] and Linhan Lin[1*]

*Correspondence:
hbsun@tsinghua.edu.cn;
linlh2019@mail.tsinghua.edu.cn

[1] State Key Laboratory of Precision Measurement Technology and Instruments, Department of Precision Instrument, Tsinghua University, Beijing 100084, China
[2] State Key Laboratory of Integrated Optoelectronics, College of Electronic Science and Engineering, Jilin University, Changchun 130012, China

Abstract
Waveguide quantum electrodynamics (QED) system manifests an ideal platform for studying many-body physics. When multiple emitters are coupled to a common waveguide, subradiant states may arise because of the waveguide-mediated interaction, leading to a long lifetime because of their immunity to the waveguide mode-induced dissipation. However, they can still be influenced by local environments, which are incoherent for different emitters and cannot be canceled out through interference. Herein, a new mechanism termed energy quantum confinement effect (EQCE) is proposed in a non-Markovian waveguide QED system to suppress the local dissipation. The energy quantum is confined in the waveguide by emitters, suppressing spontaneous decay of the emitters. The EQCE makes the system partly free from local dissipation of emitters, leading to a total decay rate lower than the local decay rate. We further show that similar effect occurs spontaneously by self-interference and can be stressed by cooperative coupling, relaxing the requirement for initializing the emitters into a remotely entangled state.

Keywords: Waveguide QED, Subradiant state, Non-Markovian quantum process

Introduction

Spontaneous emission roots in the quantum nature of the electromagnetic (EM) field [1]. For multiple emitters coupled to common EM modes (e.g., an optical waveguide or an optical cavity), the emission processes of different emitters are not independent, but interfere with each other to yield super- or sub-radiance when the interference is constructive or destructive, respectively [2–10]. Specifically, subradiant states are long-lived entangled states, and emitters in subradiant states are promising candidates for long-lifetime qubits, or quantum memory [11–15], and can also be useful for quantum metrology [16–18].

Waveguide quantum electrodynamics (QED) has emerged as an ideally suited quantum system for investigating collective emitter-photon interactions [2, 19–29]. In waveguide QED, subradiant states can be prepared by optical excitation which endows the emitters desired phases from the photons, or naturally arise as steady states of collective decay process [7, 16]. Unlike the conventional approach with an ensemble of emitters, the infinite emitter-emitter interaction length and strong emitter-photon interaction strength allow subradiance from spatially separated emitters, permitting individual addressing [5, 6, 29]. However, as only the influence of the *shared EM modes* can be suppressed by interference cancellation, the subradiant state can still be vulnerable to *local* environments. For instance, when an emitter A is coupled to a one-dimensional (1D) waveguide, its total decay rate can be written as $\gamma = \gamma_{1D} + \gamma_0$, where γ_{1D} is the decay rate caused by the 1D waveguide and γ_0 is the decay rate caused by the vacuum free space. The γ_{1D} part of the total decay rate can be suppressed by coupling another emitter B to this waveguide, where the influences of the waveguide mode on these two emitters cancel with each other. However, the γ_0 part always exists and cannot be suppressed by interference cancellation, because the vacuum EM modes felt by emitters A and B have no correlations [16, 30–34]. Thus, γ_0 can be considered as the decay rate of a subradiant state and sets a lower bound of the total decay rate $\gamma \gtrsim \gamma_0$. Such a limit of the decay rate leads to the theoretical limits of qubit lifetime, the fidelity of quantum state preparation, and sensitivity in entangled state metrology, etc. [11, 12, 35]

Here we propose to break this physical limit by designing a waveguide QED system in the non-Markovian regime [36–40], where the total decay rate $\gamma < \gamma_0$ stems from the retarded interaction [41–44] and the energy quantum confinement effect (EQCE). The term "energy quantum" refers to the quantized energy $E = \hbar\omega_0$ associated with the transition between the excited and ground states of the emitters coupled to the waveguide, which is not necessarily stored in a single photon or in the excited states of the emitters, but can also be stored in a superposition of them. A photon emitted by one emitter propagates along a waveguide for nonnegligible time T before interacting with another emitter. The energy quantum is partly stored in the propagating photons, and the interference with another emitter protects the propagating photon from being coupled to the scattering modes of the waveguide. The EQCE makes the system partly immune from local emission of emitters to the free space, thus leading to a total decay rate lower than γ_0. More interestingly, we show that similar effect arises in a system with time-delayed feedback, where the emitter is fed by its historical version and the ultra-small decay rate originates from self-interference. The emitter can be replaced by a collection of emitters, where the cooperative emission improves the atom-waveguide coupling efficiency, thus magnifying the local-decay suppression effect.

Results and discussion

Theoretical model

As schematically illustrated in Fig. 1a, two identical emitters, A at x_A and B at x_B, with a central transition frequency ω_0 are coupled to a common 1D waveguide with inter-emitter distance Δx. The emitters are described by the Pauli operators $\sigma_i = |g\rangle_{ii}\langle e|$ and $\sigma_i^+ = |e\rangle_{ii}\langle g|$, where $|g\rangle_i$ and $|e\rangle_i$ are the ground and excited states of emitter i for $i \in \{A, B\}$. The spatial distance Δx thus set a temporal distance $T = \Delta x / v_g$ for the emitters, i.e., the impact of one emitter on the other is retarded by T. Here v_g is the group velocity of a wave packet with central frequency ω_0. The waveguide EM modes at frequency ω are described by the annihilation (creation) operators $a_{R,\omega}$ $(a^\dagger_{R,\omega})$ and $a_{L,\omega}$ $(a^\dagger_{L,\omega})$ for the right- and left-propagating photons, respectively. The 1D waveguide is assumed to be bidirectional, i.e., each emitter

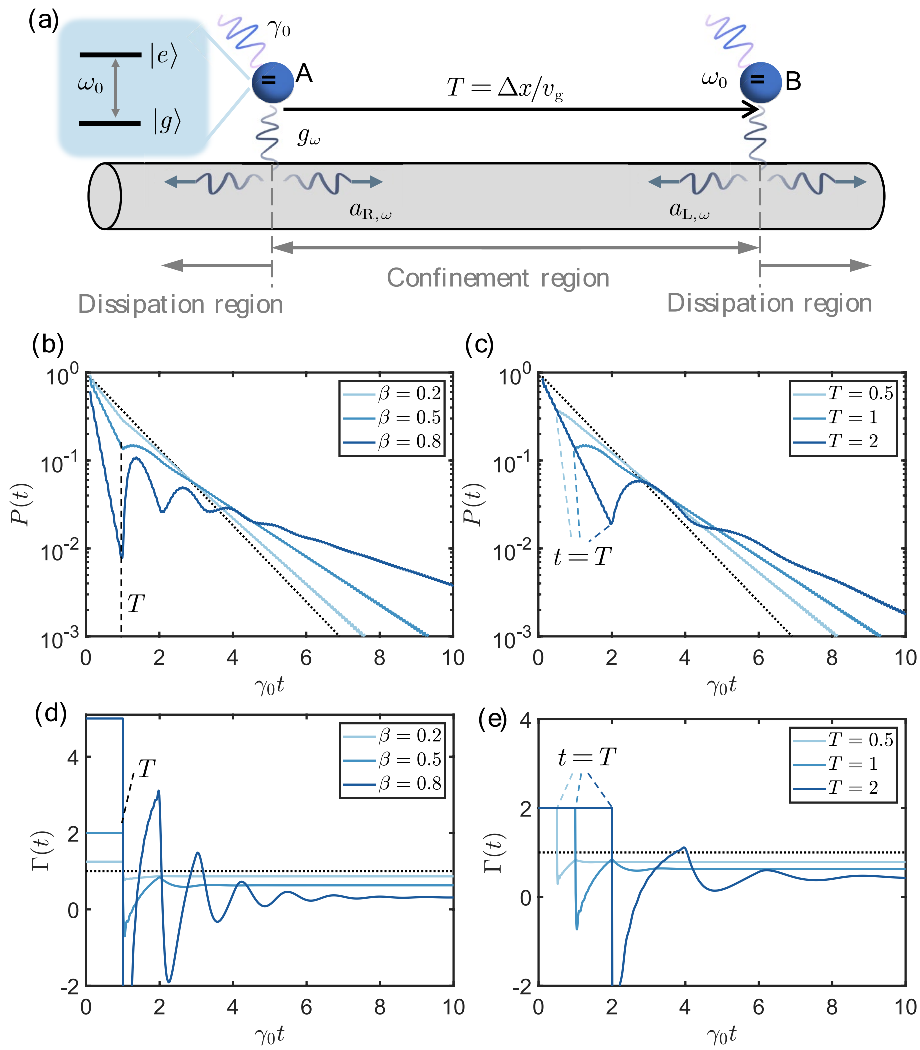

Fig. 1 **a** Setup and coupling scheme. Two identical two-level emitters A and B with distance Δx are coupled to a common 1D waveguide. Emitter excitation probability $P(t)$ versus time (in units of $1/\gamma_0$) in semi-logarithmic coordinate **b** for different coupling efficiencies β and **c** for different inter-atom temporal distances T. We set $T=1$ in **b** and $\beta=0.5$ in **c**, respectively, and $\gamma_0=1$ is kept unchanged in all cases. The black dotted line for exponential decay $P(t)=\exp(-\gamma_0 t)$ is plotted for comparison. **d-e** Emitter instantaneous decay rate Γ versus time corresponding to **b** and **c**, respectively

couples to the waveguide EM mode of frequency ω with strength g_ω regardless of the propagation direction.

With the clear description of the emitter-waveguide coupling, we obtain the full Hamiltonian $H=H_0+H_{\text{int}}$ governing the dynamics of the system, where ($\hbar=1$)

$$H_0=\omega_0\sum_{i\in\{A,B\}}\sigma_i^+\sigma_i+\int_0^\infty d\omega\,\omega\left(a_{R,\omega}^\dagger a_{R,\omega}+a_{L,\omega}^\dagger a_{L,\omega}\right), \tag{1}$$

$$H_{\text{int}}=\sum_{i\in\{A,B\}}\int_0^\infty d\omega\left(g_\omega\sigma_i^+a_{R,\omega}e^{ik_\omega x_i}+g_\omega\sigma_i^+a_{L,\omega}e^{-ik_\omega x_i}+\text{H.c.}\right). \tag{2}$$

Note that although there can be different values of ω_k with respect to the same wavevector k, one can safely consider only the $\omega_k \simeq \omega_0$ mode because for other modes the coupling strengths with the two-level emitters is negligible. At $t = 0$, the waveguide is assumed to be in the vacuum state such that $\langle a^{\dagger}_{\mathrm{R},\omega} a_{\mathrm{R},\omega}\rangle = \langle a^{\dagger}_{\mathrm{L},\omega} a_{\mathrm{L},\omega}\rangle = 0$, and the emitters are assumed to be in the antisymmetric superposition state (the so-called *dark state* [4, 33]) $|D\rangle = \left(|eg\rangle - |ge\rangle\right)/\sqrt{2}$. For $t > 0$, the emitters are coupled to the waveguide and the time-evolving state can be written as

$$|\psi(t)\rangle = \sum_{i\in\{\mathrm{A},\mathrm{B}\}} c_i(t)\sigma_i^{+}|G,0\rangle + \int_0^{\infty} \mathrm{d}\omega \left[c_{\mathrm{R},\omega}(t)a^{\dagger}_{\mathrm{R},\omega} + c_{\mathrm{L},\omega}(t)a^{\dagger}_{\mathrm{L},\omega}\right]|G,0\rangle, \tag{3}$$

where $c_i(t)$ is the probability amplitude of emitter i at excited state and $c_{\mathrm{R/L},\omega}(t)$ is the amplitude of the right-/left-propagating waveguide mode with frequency ω. $|G,0\rangle$ denotes the state where all emitters are in the ground state and the EM field is in the vacuum state.

After tracing off the degrees of freedom of the waveguide, and considering the free space EM modes induced local decay rate γ_0, the equation of motion for emitter $i \in \{\mathrm{A}, \mathrm{B}\}$ is derived to be (see Supplementary Information for details)

$$\dot{c}_i(t) = -\frac{\gamma}{2}\left[c_i(t) + \beta c_{j\neq i}(t-T)\mathrm{e}^{\mathrm{i}\varphi}\Theta(t-T)\right]. \tag{4}$$

Here $\gamma = \gamma_0 + \gamma_{1\mathrm{D}}$ is the total decay rate of an individual emitter, where $\gamma_{1\mathrm{D}} = 2\int_0^{\infty}|g_\omega|^2\mathrm{d}\omega$ denotes the waveguide EM modes induced decay rate and $\beta = \gamma_{1\mathrm{D}}/\gamma$ is the coupling efficiency. $\varphi = \omega_0\Delta x/v_{\mathrm{g}}$ is the photon propagation phase between sites A and B. In what follows we assume that the emitters are positioned such that $\mathrm{e}^{\mathrm{i}\varphi} = 1$, which guarantees that the dark state $|D\rangle$ coincides with the subradiant state in the Markovian regime if the retardation T is ignorable [5, 6]. The Heaviside step function $\Theta(t-T)$ shows explicitly that the influence of one emitter on the other is retarded by T, before which the emitters decay exponentially as if there were only one emitter.

Non-Markovian subradiant state

The time evolution of the dark state $|D\rangle$ can be obtained by solving Eq. [4] analytically, as detailed in the Supplementary Information. In Fig. 1b-c, the total excited state population $P(t) = \sum_{i\in\mathrm{A,B}}|c_i(t)|^2$ is shown under different coupling efficiencies β between the emitters and the waveguide and at different retardation T, respectively. Note that for different coupling strengths between the emitters and the waveguide, $\gamma_{1\mathrm{D}}$ varies accordingly, whereas γ_0 keeps unchanged. Thus, different values of β can be obtained with the same value of γ_0. To capture the main feature of the dark state evolution, we introduce the excited-state decay rate $\Gamma(t) := -(\mathrm{d}/\mathrm{d}t)\ln P(t)$ in Fig. 1d-e. The behaviors of $\Gamma(t)$ are quantitatively separated into two regimes and highlight the abrupt transition at $t = T$. (1) Spontaneous decay regime ($t < T$): $\Gamma(t) \equiv \gamma$, reflecting independent emitter decay because the influence of the emitters on each other is retarded by T. (2) Quasi-BS regime ($t > T$): $\Gamma(t)$ oscillates shortly after $t = T$ and then rapidly converges to a steady-state value.

We attribute the oscillations to photon reabsorption and interference, which gradually stabilize the system into the suppressed decay regime. As can be seen from Fig. 1 d-e, at $t = T + 0^+$, the instantaneous decay rate $\Gamma(t)$ jumps to smaller values (even negative values for large β and/or T). A negative decay rate means the increase of excited-state emitter population and is attributed to photon reabsorption, in consistence with the time T needed for photon propagation between two emitters. For $t \in [T, 2T]$, $\Gamma(t)$ keeps increasing because of the reduced EM field intensity as the EM field emitted from the other emitter keeps decreasing when $t \in [0, T]$. On the other hand, when $\Gamma(t)$ has negative values, the increase of $\Gamma(t)$ also arises from the stimulated emission: For an emitter with probability $P_e = |c_e|^2$ in the excited state and $P_g = 1 - |c_e|^2$ in the ground state, stimulated emission and stimulated absorption co-exist; when interacting with photons, a larger P_e will improve the influence of stimulated emission and consequently increase $\Gamma(t)$. At $t = 2T + 0^+$, $\Gamma(t)$ decreases abruptly because of sudden increment of the EM field intensity, which is caused by the arrival of reflected photons after a round-trip between emitters. Similar considerations apply for $t = nT + 0^+$, $n = 3,4,5 \cdots$ when photons bounce between emitters for different cycles. Notably, the amplitudes of oscillations increases with the coupling efficiency β and the (temporal) distance T, both of which lead to lower excited population $P(t)$ of the emitters and hence magnifies the influence of reabsorption; a higher coupling efficiency β also boosts the oscillation because of the increased EM field intensity absorbed by the emitters.

As we fix the decay rate into the free space γ_0 unchanged, a higher coupling efficiency β means a higher decay rate into the waveguide and hence a higher total decay rate γ, as evidenced in Fig. 1b when $t < T$. However, when $t > T$, the population $P(t)$ decays *slower* with larger β as a result of the enhanced EQCE. In Fig. 1c, it is noticed that a longer retardation T also leads to a lower decay rate when $t > T$, even though the *local* coupling parameter remains unchanged. Specifically, in the case that the retardation T is small, we obtain (see Supplementary Information)

$$\Gamma \simeq \frac{1}{1 + \gamma_{1\mathrm{D}} T/2} \gamma_0. \tag{5}$$

Although Eq. [5] is mathematically solid only when T is small, it captures the main features of Γ when $t > T$ that Γ decreases monotonically with both β (and consequently $\gamma_{1\mathrm{D}}$) and T. When $T \to 0$, we have $\Gamma \to \gamma_0$, as is the result of the well-studied Markovian situation [2, 6, 45].

To gain insight into this non-Markovian local-decay suppression effect, we calculated the EM field intensity $I(x, t)$ in the Supplementary Information, and the results for different β are presented in Fig. 2. Let us focus on Fig. 2a-b first. When $t \in (0, T/2)$, the emitters at x_A and x_B emit independently, from which the EM fields propagate bidirectionally. At $t = T/2$, EM fields emitted from x_A and x_B begin to interfere with each other. When $t = T$, the EM field emitted from x_A arrives at from x_B and photon reabsorption occurs, in consistence with the results in Fig. 1b-c. It is noted that the EM fields emitted when $t > T$ are mainly localized in $x \in (x_\mathrm{A}, x_\mathrm{B})$, outside which the EM field vanishes because of the destructive interference between the EM fields emitted by different emitters.

Actually, the steady state of our system corresponds to an emitter-photon bound state (BS) if $\gamma_0 = 0$ [41, 46, 47]. When $\gamma_0 \neq 0$, the steady state at $t > T$ is not perfectly bounded, but quasi-bounded. The energy of this quasi-BS is partly confined in

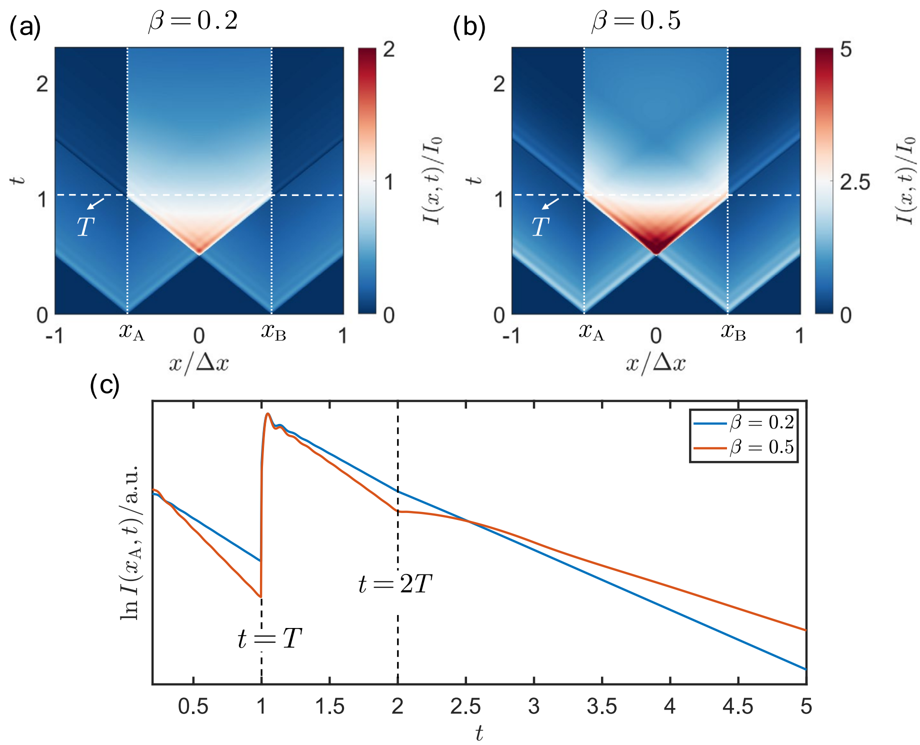

Fig. 2 EM field intensity as a function of position and time for **a** $\beta = 0.2$ and **b** $\beta = 0.5$, respectively. Emitters A and B are positioned at x_A and x_B, respectively, and are marked by the vertical dotted lines. Time $t = T$ is marked by horizontal dashed lines. We set $T = 1$ and $\gamma_0 = 1$ in both cases. Pay attention to the different color bars. **c** Normalized EM field intensity at $x = x_A + 0^+$. Times $t = T$ and $t = 2T$ are marked by vertical dashed lines

the EM field in $x \in (x_A, x_B)$, which is totally free from dissipation if the propagation loss is negligible. The energy stored in the excited emitters, on the other hand, suffer from local spontaneous decay with the decay rate of γ_0. However, the local dissipation of the emitters is continuously compensated by the EM field, thus leading to an ultra-small excited state decay rate $\Gamma < \gamma_0$. As illustrated in Fig. 2a-b: when $t < T$, the higher coupling efficiency β, the more energy emitted into the EM field in $x \in (x_A, x_B)$; when $t > T$, the field intensity decreases slower because more energy is stored in the EM field (consequently a small fraction of the EM field energy is able to compensate for the local dissipation of the emitters). This is clearly shown in Fig. 2c, where the field intensity at $x_A + 0^+$ (i.e., adjacent to the right side of x_A) is plotted. The larger slope is observed at $\beta = 0.5$ than the case of $\beta = 0.2$ when $t < T$, which means a faster decay of the emitters. The slopes change at $t = 2T$ because of the arrival of the emitter B-reflected field that is emitted by emitter A at $t = 0$. This change is only obvious when β is large because the emitter-induced reflectivity is an increasing function of β [2, 19]. The dependency of effective decay rate Γ on the retardation T can be similarly considered, which determines how long the emitters decay independently before the establishment of the quasi-BS.

Since the overlap of the initial state $|\psi(0)\rangle$ with the quasi-BS is low, there is a considerable reduction of excitation probability P at the spontaneous decay regime (i.e.,

$t < T$). Notably, such a low excitation probability could be significantly overcome if the quasi-BS could be prepared without the spontaneous decay regime. A highly efficient protocol for preparing the quasi- BS has been demonstrated in ref. [46]. By engineering structured photon wave-packets and harnessing multiphoton nonlinear scattering, the excitation-emission reciprocity is broken and the quasi-BS can be directly excited at a high probability of $P_{\text{tr}} \approx 0.8$, marking a significant improvement in practical implementations. Here we have adopted a simplified approach that leverages spontaneous emission to generate quasi- BS, as a comprehensive exploration of quasi-BS excitation methods extends far beyond the scope of this study.

Self-interference and cooperative emission

In the above-described approach to the non-Markovian BS through EQCE, one has to initialize two remote emitters in the antisymmetric entangled state, which may set obstacles for experimental realization. However, the concept of EQCE is not limited by using two entangled emitters. Here we show that the BS can be established when only one emitter is initially excited while the other remains in the ground state. Moreover, each emitter can be replaced by a collection of emitters and magnifies the decay-rate suppression effect by cooperative emission.

As displayed in Fig. 3a, now we consider the waveguide formed by a 1D array of N tunnel-coupled cavities [47–50]. Such a waveguide configuration facilitates the modeling of multiple emitters coupled to the same site, and is suitable for the investigation of local cooperative emission. The cavity array is described by a tight-binding Hamiltonian

$$H_{\text{ph}} = \sum_{x=1}^{N} \omega_{\text{c}} a_x^\dagger a_x - J \sum_{x=1}^{N-1} \left(a_{x+1}^\dagger a_x + a_x^\dagger a_{x+1}\right), \tag{6}$$

where a_x is the photon annihilation operator of cavity x, $J > 0$ is the tunneling strength, and ω_c is the central frequency of each individual cavity, respectively. Hereafter we mainly focus on the on-resonance situation where $\omega_c = \omega_{\text{A}} = \omega_{\text{B}}$, with ω_{A} and ω_{B} the transition frequencies of the two collection of emitters (each collection with N_i emitters) in cavity x_{A} and x_{B}, respectively. Considering the local decay rate γ_0 of the emitters, we introduce the complex transition frequency $\widetilde{\omega}_i = \omega_i - \mathrm{i}\gamma_0/2$ for emitter $i \in \{\text{A}, \text{B}\}$. Then the total Hamiltonian reads

$$H = H_{\text{ph}} + \sum_{\substack{i \in \{\text{A},\text{B}\} \\ j \leq N_i}} \left[\widetilde{\omega}_i \sigma_{i,j}^+ \sigma_{i,j} + \left(g_i a_{x_i}^\dagger \sigma_{i,j} + \text{H.c.}\right)\right]. \tag{7}$$

Instead of an entangled initial state, here we assume that only one emitter in cavity x_{A} is excited at $t = 0$. Without loss of generality we assume $\left|\psi(0)\right\rangle = \sigma_{\text{A},1}^+ \left|G, 0\right\rangle$. At time t the state has the following form

$$|\psi(t)\rangle = \left(\sum_{i,j} c_{i,j}(t)\sigma_{i,j}^+ + \sum_x c_x(t) a_x^\dagger\right)|G, 0\rangle \tag{8}$$

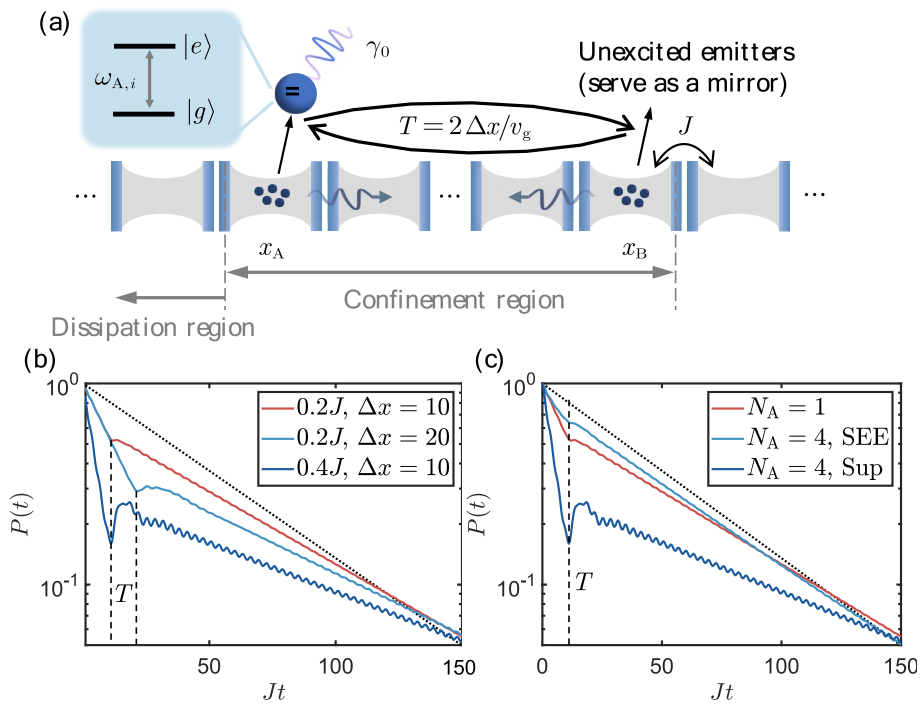

Fig. 3 **a** Sketch of the waveguide consisting of tunnel-coupled cavities, where J is the tunneling strength between neighboring cavities. Two collections of emitters are coupled to cavities at x_A and x_B, each with N_A and N_B emitters, respectively. T sets a lower time bound for a photon to have a round trip between x_A and x_B. Emitter excitation probability $P(t)$ versus time (in units of $1/J$) are plotted in semi-logarithmic coordinate **b** for different coupling strengths $g_A = 0.2J, 0.4J$ or different inter-emitter distances $\Delta x = 10, 20$ and **c** for different number of emitters at x_A. For $N_A = 4$, different initial state is considered, where there is only a single excited emitter (denoted by "SEE") or the initial state is in the superradiant state (denoted by "Sup"). We set $N_A = 1$ in **b** and $g_A = 0.2J, \Delta x = 10$ in **c**, respectively, and $\sqrt{N_B} g_B = 2J$ is kept unchanged in all cases. The black dotted line for exponential decay $P(t) = \exp(-\gamma_0 t)$ is plotted for comparison

where $c_{i,j}(t)$ is the probability amplitude of emitter j in cavity x_A being excited and $c_x(t)$ the probability amplitude of one photon being located at cavity x. We calculate the evolution of the system directly by solving the Schrödinger's equation $i\partial_t|\psi(t)\rangle = H|\psi(t)\rangle$. The excited state population $P(t) = \sum_j |c_{A,j}(t)|^2$ is presented in Fig. 3b-c. When $t < T$ (T is the time needed for the self-interference to establish, and the exact value of T will be specified later), $P(t)$ decays exponentially with rate $\gamma = \gamma_0 + \gamma_{1D}$, with now $\gamma_{1D} = g_A^2/J$ [48]. At time $t = T$, the x_B-reflected EM field begins to arrive at x_A, and the quasi-BS forms by *self-interference*, thus reducing the total decay rate.

In order to evaluate the time scale needed for this delayed feedback [51–54], the cavity modes are Fourier-transformed to the momentum representation (k-space) where $a_k = \left(1/\sqrt{N}\right)\sum_x a_x \exp(ikx)$, $g_i^k = \left(1/\sqrt{N}\right) g_i \exp(ikx_i)$ and $\omega_k = \omega_c - 2J\cos k$ (see Supplementary Information). The waveguide dispersion relation gives rise to the peak group velocity $v_g^m = \max\{d\omega_k/dk\} = 2J$ at $k_m = \pm\pi/2$. Consequently, we have $T \sim 2\Delta x/v_g^m$, the time that must be spent before the reflected fields arrive. We set Δx to be an even integer, i.e., $\Delta x = 2n,\ n \in \mathbb{Z}$, which yields a propagating phase of $\sim 2\Delta x|k_m|d = 2n\pi$; combined with the π shift induced by total reflection at cavity x_B, the total accumulated phase in one round trip between x_A and x_B is $\phi = (2n+1)\pi$, thus leading to a destructive interference at cavity x_A [44].

In Fig. 3b, the dependence of $P(t)$ on different inter-emitter distances Δx (consequently different retardation T) and different emitter-cavity coupling strengths (consequently different coupling efficiency β) is displayed. The results can be similarly understood as that in Fig. 1b-c. The situations are different when we consider a collection of emitters in the cavity. In Fig. 3c, the results for $N_A = 1, 4$ are presented. For $N_A = 4$, if there is only a single excited emitter (denoted by "SEE") initially, the excited state decay rate $\Gamma(t)$ is suppressed when $t < T$ compared to the $N_A = 1$ case, which stems from the reabsorption, i.e., the emitted photon can be absorbed by other emitters before tunneling into neighboring cavities. On the contrary, $\Gamma(t)$ is larger than that of $N_A = 1$ when $t > T$, which we attribute to the reabsorption induced phase mismatch: destructive interference occurs between one emitter at time t and the photon emitted at $t - T$. When reabsorption exists, a photon takes longer time than T for a round trip between x_A and x_B because of the time spent among emitters in cavity x_A. In order to avoid the reabsorption, we thus prepare the initial state in the superradiant state (denoted by "Sup") $\left|\psi(0)\right\rangle = (1/2)\sum_{i=1}^{4}\sigma_{A,i}^{+}\left|G, 0\right\rangle$. It is seen that the excited-state decay rate $\Gamma(t)$ is firstly improved when $t < T$ because of the local superradiance, and then suppressed when $t > T$ because of the improved coupling efficiency, as have been discussed in the two-emitter case.

In the self-interference model, emitters in cavity x_B serve as a mirror [55–58] and reflect the EM field. In all our calculations, we have kept $\sqrt{N_B}g_B = 2J$ unchanged, as the reflection is determined by $\sqrt{N_B}g_B$ (see Supplementary Information), i.e., the number of emitters and the emitter-cavity coupling strength. When the reflected field arrives at cavity x_A, it interferes destructively with the real-time emitted field and thus the EM fields are confined between x_A and x_B, as displayed in Fig. 4. It is shown that after the right-propagating field arrives at x_B, the reflected field begins to interfere with the unreflected field to form a standing wave. Emitters at x_A and x_B are the nodes of this wave, and the system mimics the so-called vacancy-like dressed states [57, 58]. The confined EM field compensates for the emitter dissipation similar to the case discussed in Fig. 2.

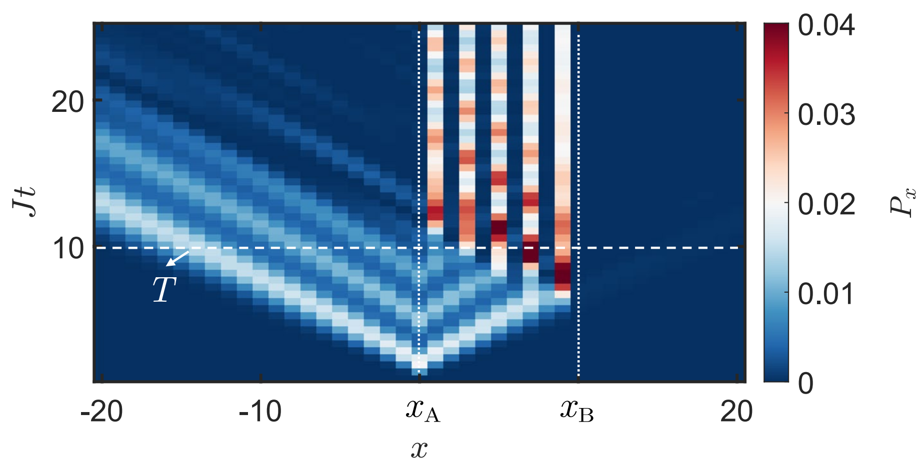

Fig. 4 Photon distribution probability $P(x) = |c_x|^2$ as a function of position and time

Notably, alternative approaches may exist for controlling spontaneous emission processes. For instance, photonic bandgap structures have been extensively studied for their ability to inhibit spontaneous emission through local density-of-states (LDOS) engineering. Alternatively, in free space configurations, strategic application of external electromagnetic fields to atomic systems with tailored energy levels has demonstrated suppression effects. Photonic crystals suppress spontaneous emission by creating a photonic bandgap that prohibits photon emission at specific frequencies due to a vanishing LDOS [59, 60]. While efficient spontaneous emission suppression can be achieved for emitters resonant with the bandgap, it imposes stringent requirements on spectral alignment and nanostructural precision. The fixed bandgap positions and fabrication challenges in integrating emitters into periodic lattices severely limit its scalability and tunability [61]. External-field control techniques, such as electromagnetically induced transparency (EIT), exploit dark states to suppress emission by dressing emitter transitions with external fields [62, 63]. Although dynamically tunable via external parameters (e.g., laser intensity, detuning), these methods demand stable high-power lasers and specific level schemes (e.g., Λ- or V-type configurations), rendering them susceptible to decoherence from environmental noise and impractical for scalable quantum networks [64].

Critically, strategies such as photonic bandgap engineering and external field control primarily target single-emitter systems, limiting their applicability in scenarios requiring multiqubit coherence preservation—a fundamental demand in quantum computing. For such systems, leveraging interference-cancellation mechanisms to protect qubits aligns more naturally with the intrinsic requirements of quantum computation, which inherently involves the manipulation of multipartite entangled states. In this context, the dark state, or more broadly speaking, the decoherence-free subspace (DFS) offers a distinct advantage: their construction inherently relies on (anti) symmetric multiqubit state, which are topologically compatible with multiqubit gate operations [12, 65]. This structural synergy makes DFS particularly effective for safeguarding entangled states, as their symmetry-driven design directly mirrors the collective dynamics essential to quantum algorithms. However, the γ_0 part always exists and cannot be suppressed by interference cancellation in conventional DFS engineering, which brings us the motivation of us to break this physical limit.

Our approach leverages the EQCE, where delayed feedback and interference in a waveguide-QED system suppress spontaneous emission below the free-space decay rate. This is achieved without requiring bandgap alignment or external fields, as the waveguide inherently channels photons into guided modes while non-Markovian dynamics stabilizes the quasi-BS. Emitters can be individually addressed at tunable positions, facilitating integration into on-chip quantum networks. The EQCE is immune to free-space LDOS fluctuations and requires no active field stabilization, outperforming EIT in noisy environments. On the other hand, these approaches to spontaneous emission are compatible and hybrid approaches could further enhance performance. Combining periodic structures with waveguide QED could improve the coupling efficiency, amplifying the EQCE. Integrating external fields with waveguide-QED systems may enable real-time control of Γ and T.

Our proposal can be applied in a concrete design given in Fig. S1, Supplementary Information, i.e., two Cs atoms (with D_1 transition at 894.6 nm) are coupled to 1D alligator photonic crystal waveguides which are linked by an optical fiber. According to ref. [20], $\gamma_{1D}/\gamma_0 \approx 1$ could be obtained, leading to a coupling efficiency of $\beta \approx 0.5$. With the reported value $\gamma_0 \approx 2\pi \times 4.56$ MHz, the retardation time between two atoms T satisfying $\gamma_0 T = 1$ is $T \approx 34.9$ ns. Such a long retardation time required for the non-Markovian effect has also been accessible. In another experiment using Cs atoms [23], 5.843(5) m and 45.423(5) m fibers were used to provide retardation times of 28.26(3) ns and 219.70(3) ns, respectively. The excited state population as a function of time in such a system is included in Fig. 1 b at $\beta = 0.5$. Regarding the experimental viability, each single atom can also be replaced by an atomic ensemble with low average atom numbers to improve the feasibility. Initializing the ensembles into superradiant states can further boost the coupling efficiency, thereby magnifying the EQCE-induced suppression of local decay.

Conclusion

In summary, we have proposed a new physical mechanism termed EQCE, i.e., confinement of energy quantum in a waveguide by emitters, to efficiently suppress the local dissipation of emitters. A total decay rate lower than the local decay rate of individual emitters is obtained, which is imparted by the retarded interaction and vanishes in the Markovian regime. Such decay-suppression effect can be boosted by increasing the inter-emitter distance and the coupling efficiency. It occurs spontaneously in a self-interference setup, and can be stressed by local superradiance. We anticipate that non-Markovian subradiant states could yield new error bounds and protocols for many applications in quantum technology, ranging from quantum memory to quantum metrology. The non-Markovian collective states itself could also constitute a new realm with rich many-body physics.

Supplementary Information

The online version contains supplementary material available at https://doi.org/10.1186/s43074-025-00167-6.

Supplementary Material 1.

Acknowledgements

L.L. acknowledges support from the National Key Research and Development Program of China (grant 2020YFA0715000), the National Natural Science Foundation of China (grant 62075111), and the Tsinghua University Initiative Scientific Research Program; H.-B.S. acknowledges support from the National Natural Science Foundation of China (grant 61960206003) and Tsinghua-Foshan Innovation Special Fund (grant 2021THFS0102).

Authors' contributions

Y. L conceived the idea and developed the theoretical analysis. Y. L and L. L. prepared the preliminary manuscript. H.-B. S. and L. L supervised the project. All authors participated in discussions and contributed to the editing of the article.

Data availability

The data sets generated and/or analyzed during this study are available from the corresponding authors on reasonable request.

Declarations

Competing interests

The authors declare the following competing interests: H.-B. Sun serves as a Co-Editor-in-Chief of PhotoniX; L. Lin is an Associate Editor of PhotoniX. Both were excluded from editorial handling of this manuscript.

Received: 9 January 2025 Revised: 11 March 2025 Accepted: 18 March 2025
Published online: 31 March 2025

References

1. Scully MO, Zubairy MS. Quantum Optics. Cambridge University Press; 1997.
2. Sheremet AS, Petrov MI, Iorsh IV, Poshakinskiy AV, Poddubny AN. Waveguide quantum electrodynamics: Collective radiance and photon-photon correlations. Rev Mod Phys. 2023;95: 015002.
3. Reitz M, Sommer C, Genes C. Cooperative quantum phenomena in light-matter platforms. PRX Quantum. 2022;3: 010201.
4. Evans RE, et al. Photon-mediated interactions between quantum emitters in a diamond nanocavity. Science. 2018;362:662.
5. van Loo AF, Fedorov A, Lalumière K, Sanders BC, Blais A, Wallraff A. Photon-mediated interactions between distant artificial atoms. Science. 2013;342:1494.
6. Tiranov A, et al. Collective super- and subradiant dynamics between distant optical quantum emitters. Science. 2023;379:389.
7. González-Tudela A, Paulisch V, Chang DE, Kimble HJ, Cirac JI. Deterministic generation of arbitrary photonic states assisted by dissipation. Phys Rev Lett. 2015;115:163603.
8. Norcia MA, Winchester MN, Cline JRK, Thompson JK. Superradiance on the millihertz linewidth strontium clock transition. Sci Adv. 2016;2: e1601231.
9. Zhou X, Tamura H, Chang T-H, Hung C-L. Trapped atoms and superradiance on an integrated nanophotonic microring circuit. Phys Rev X. 2024;14: 031004.
10. Liu Y, Zhou H, Xue P, Lin L, Sun H-B. Photoswitchable quantum electrodynamics in a hybrid plasmonic quantum emitter. Chip. 2023;2: 100060.
11. Sangouard N, Simon C, de Riedmatten H, Gisin N. Quantum repeaters based on atomic ensembles and linear optics. Rev Mod Phys. 2011;83:33.
12. Suter D, Álvarez GA. Colloquium: Protecting quantum information against environmental noise. Rev Mod Phys. 2016;88: 041001.
13. Zanardi P, Rasetti M. Noiseless quantum codes. Phys Rev Lett. 1997;79:3306.
14. Facchinetti G, Jenkins SD, Ruostekoski J. Storing light with subradiant correlations in arrays of atoms. Phys Rev Lett. 2016;117: 243601.
15. Asenjo-Garcia A, Moreno-Cardoner M, Albrecht A, Kimble HJ, Chang DE. Exponential improvement in photon storage fidelities using subradiance and "selective radiance" in atomic arrays. Phys Rev X. 2017;7: 031024.
16. Piñeiro Orioli A, Thompson JK, Rey AM. Emergent dark states from superradiant dynamics in multilevel atoms in a cavity. Phys Rev X. 2022;12:011054.
17. Zhang C, Yu P, Jadbabaie A, Hutzler NR. Quantum-enhanced metrology for molecular symmetry violation using decoherence-free subspaces. Phys Rev Lett. 2023;131: 193602.
18. DeMille D, Hutzler NR, Rey AM, Zelevinsky T. Quantum sensing and metrology for fundamental physics with molecules. Nat Phys. 2024;20:741.
19. Roy D, Wilson CM, Firstenberg O. Colloquium: Strongly interacting photons in one-dimensional continuum. Rev Mod Phys. 2017;89: 021001.
20. Goban A, Hung C-L, Hood JD, Yu S-P, Muniz JA, Painter O, Kimble HJ. Superradiance for atoms trapped along a photonic crystal waveguide. Phys Rev Lett. 2015;115: 063601.
21. Pennetta R, Blaha M, Johnson A, Lechner D, Schneeweiss P, Volz J, Rauschenbeutel A. Collective radiative dynamics of an ensemble of cold atoms coupled to an optical waveguide. Phys Rev Lett. 2022;128: 073601.
22. Liedl C, Pucher S, Tebbenjohanns F, Schneeweiss P, Rauschenbeutel A. Collective radiation of a cascaded quantum system: From timed dicke states to inverted ensembles. Phys Rev Lett. 2023;130: 163602.
23. Lechner D, Pennetta R, Blaha M, Schneeweiss P, Rauschenbeutel A, Volz J. Light-matter interaction at the transition between cavity and waveguide QED. Phys Rev Lett. 2023;131: 103603.
24. Tabares C, Muñoz de Las Heras A, Tagliacozzo L, Porras D, González-Tudela A. Variational quantum simulators based on waveguide QED. Phys Rev lett. 2023;131:073602.
25. Liedl C, Tebbenjohanns F, Bach C, Pucher S, Rauschenbeutel A, Schneeweiss P. Observation of superradiant bursts in a cascaded quantum system. Phys Rev X. 2024;14: 011020.
26. Shi J, Poddubny AN. Multimer states in multilevel waveguide QED. Physical Review A. 2024;110(5). https://doi.org/10.1103/physreva.110.053707.
27. Solano P, Barberis-Blostein P, Fatemi FK, Orozco LA, Rolston SL. Super-radiance reveals infinite-range dipole interactions through a nanofiber. Nat Commun. 2017;8:1857.
28. Corzo NV, Raskop J, Chandra A, Sheremet AS, Gouraud B, Laurat J. Waveguide-coupled single collective excitation of atomic arrays. Nature. 2019;566:359.
29. Sipahigil A, et al. An integrated diamond nanophotonics platform for quantum-optical networks. Science. 2016;354:847.
30. DeVoe RG, Brewer RG. Observation of superradiant and subradiant spontaneous emission of two trapped ions. Phys Rev Lett. 1996;76:2049.
31. Masson SJ, Ferrier-Barbut I, Orozco LA, Browaeys A, Asenjo-Garcia A. Many-body signatures of collective decay in atomic chains. Phys Rev Lett. 2020;125: 263601.
32. Cipris A, Moreira NA, do Espirito Santo TS, Weiss P, Villas-Boas CJ, Kaiser R, Guerin W, Bachelard R. Subradiance with saturated atoms: Population enhancement of the long-lived states. Phys Rev Lett. 2021;126:103604.
33. Holzinger R, Gutiérrez-Jáuregui R, Hönigl-Decrinis T, Kirchmair G, Asenjo-Garcia A, Ritsch H. Control of localized single- and many-body dark states in waveguide QED. Phys Rev Lett. 2022;129: 253601.

34. Salhov A, Cao Q, Cai J, Retzker A, Jelezko F, Genov G. Protecting quantum information via destructive interference of correlated noise. Phys Rev Lett. 2024;132: 223601.
35. Degen CL, Reinhard F, Cappellaro P. Quantum sensing. Rev Mod Phys. 2017;89: 035002.
36. Dinc F, Brańczyk AM. Non-markovian super-superradiance in a linear chain of up to 100 qubits. Phys Rev Res. 2019;1: 032042.
37. Ask A, Johansson G. Non-markovian steady states of a driven two-level system. Phys Rev Lett. 2022;128: 083603.
38. Zhang Y-X. Zeno regime of collective emission: Non-markovianity beyond retardation. Phys Rev Lett. 2023;131: 193603.
39. Gaikwad C, et al. Entanglement assisted probe of the non-markovian to markovian transition in open quantum system dynamics. Phys Rev Lett. 2024;132: 200401.
40. Cilluffo D, Ferialdi L, Palma GM, Calajò G, Ciccarello F. Ciccarello. Multimode-cavity picture of non-Markovian waveguide QED. 2024. https://arxiv.org/abs/2403.07110.
41. Sinha K, Meystre P, Goldschmidt EA, Fatemi FK, Rolston SL, Solano P. Non-markovian collective emission from macroscopically separated emitters. Phys Rev Lett. 2020;124: 043603.
42. Carmele A, Nemet N, Canela V, Parkins S. Pronounced non-markovian features in multiply excited, multiple emitter waveguide QED: Retardation induced anomalous population trapping. Phys Rev Res. 2020;2: 013238.
43. Arranz Regidor S, Crowder G, Carmichael H, Hughes S. Modeling quantum light-matter interactions in waveguide QED with retardation, nonlinear interactions, and a time-delayed feedback: Matrix product states versus a space-discretized waveguide model. Phys Rev Res. 2021;3: 023030.
44. Qiao L, Gong J. Coherent control of collective spontaneous emission through self-interference. Phys Rev Lett. 2022;129: 093602.
45. Liu Y, Zhou H, Lin L, Sun H-B. Tunable single emitter-cavity coupling strength through waveguide-assisted energy quantum transfer. Light Sci Appl. 2024;13:171.
46. Calajó G, Fang Y-LL, Baranger HU, Ciccarello F. Exciting a bound state in the continuum through multiphoton scattering plus delayed quantum feedback. Phys Rev Lett. 2019;122: 073601.
47. Scigliuzzo M, Calajò G, Ciccarello F, Perez Lozano D, Bengtsson A, Scarlino P, Wallraff A, Chang D, Delsing P, Gasparinetti S. Controlling atom-photon bound states in an array of josephson-junction resonators. Phys Rev X. 2022;12: 031036.
48. Wang Z, Jaako T, Kirton P, Rabl P. Supercorrelated radiance in nonlinear photonic waveguides. Phys Rev Lett. 2020;124: 213601.
49. Bello M, Platero G, Cirac JI, González-Tudela A. Unconventional quantum optics in topological waveguide QED. Sci Adv. 2019;5:eaaw0297.
50. Notomi M, Kuramochi E, Tanabe T. Large-scale arrays of ultrahigh-q coupled nanocavities. Nat Photonics. 2008;2:741.
51. Hein SM, Schulze F, Carmele A, Knorr A. Optical feedback-enhanced photon entanglement from a biexciton cascade. Phys Rev Lett. 2014;113: 027401.
52. Grimsmo AL. Time-delayed quantum feedback control. Phys Rev Lett. 2015;115: 060402.
53. Pichler H, Zoller P. Photonic circuits with time delays and quantum feedback. Phys Rev Lett. 2016;116: 093601.
54. G. Crowder, L. Ramunno, and S. Hughes, Improving on-demand single photon source coherence and indistinguishability through a time-delayed coherent feedback, arXiv:2302.08093. 2023.
55. Tufarelli T, Ciccarello F, Kim MS. Dynamics of spontaneous emission in a single-end photonic waveguide. Phys Rev A. 2013;87: 013820.
56. Mirhosseini M, Kim E, Zhang X, Sipahigil A, Dieterle PB, Keller AJ, Asenjo-Garcia A, Chang DE, Painter O. Cavity quantum electrodynamics with atom-like mirrors. Nature. 2019;569:692.
57. Nie W, Shi T, Liu Y, Nori F. Non-hermitian waveguide cavity QED with tunable atomic mirrors. Phys Rev Lett. 2023;131: 103602.
58. Leonforte L, Carollo A, Ciccarello F. Vacancy-like dressed states in topological waveguide QED. Phys Rev Lett. 2021;126: 063601.
59. Yablonovitch E. Inhibited spontaneous emission in solid-state physics and electronics. Phys Rev Lett. 1987;58: 2059.
60. Lodahl P, Floris van Driel A, Nikolaev IS, Irman A, Overgaag K, Vanmaekelbergh D, Vos WL. Controlling the dynamics of spontaneous emission from quantum dots by photonic crystals. Nature. 2004;430:654.
61. Witzens J, Loncar M, Scherer A. Self-collimation in planar photonic crystals. IEEE J Sel Top Quantum Electron. 2002;8:1246.
62. Harris SE. Electromagnetically induced transparency. Phys Today. 1997;50:36.
63. Fleischhauer M, Imamoglu A, Marangos JP. Electromagnetically induced transparency: Optics in coherent media. Rev Mod Phys. 2005;77: 633.
64. Kimble HJ. The quantum internet. Nature. 2008;453:1023.
65. Lidar DA, Chuang IL, Whaley KB. Decoherence-free subspaces for quantum computation. Phys Rev Lett. 1998;81: 2594.

Publisher's Note